



ELSEVIER

Polymer 43 (2002) 5545–5550

polymerwww.elsevier.com/locate/polymer

Adsorption of gelatins on surfactant-free PS nanoparticles

Tengjiao Hu^a, Jun Gao^b, Helmut Auweter^c, Ruediger Iden^c, Erik Lueddecke^d, Chi Wu^{a,b,*}^a*The Open Laboratory of the Bond-selection Chemistry, Department of Chemical Physics, University of Science and Technology of China, Hefei, Anhui 230026, People's Republic of China*^b*Department of Chemistry, The Chinese University of Hong Kong, Shatin, N.T., Hong Kong, People's Republic of China*^c*Department of Solid State Physics and Polymer Physics, BASF AG, Ludwigshafen, Rhine, Germany*^d*Department of Fine Chemistry, BASF AG, Ludwigshafen, Rhine, Germany*

Received 4 April 2002; received in revised form 23 May 2002; accepted 29 May 2002

Abstract

The adsorption of gelatin chains on polystyrene (PS) latex nanoparticles was investigated by a combination of static and dynamic laser light scattering (LLS). The average mass of gelatin adsorbed on each nanoparticle (m_{adsorbed}) was calculated from the absolute scattered intensity, while the hydrodynamic volume (V_{shell}) of the adsorbed gelatin layer was obtained by dynamic LLS. In pure water, due to long-range electrostatic interaction, gelatin can act as stabilizer or flocculants, depending on the length, type and concentration of gelatin chains used. We found that in pure water, $V_{\text{shell}} \propto m_{\text{adsorbed}}$; while in 2 wt% formamide aqueous solution, $V_{\text{shell}} \propto (m_{\text{adsorbed}})^2$, indicating the shifting of the dominate interaction from electrostatic to hydrophobic. The adsorption was saturated at $\sim 2 \text{ mg/m}^2$, nearly independent of pH and temperature. For a saturated adsorption, V_{shell} increases as the gelatin chain length increases. Our results indicate that the B-type gelatin with a lower molar mass and the pH range 7–9 are better choices for the stabilization of the nanoparticles in pure water. © 2002 Elsevier Science Ltd All rights reserved.

Keywords: Gelatins; Adsorption; Nanoparticles

1. Introduction

Gelatin is a mixture of multiple polypeptide strands arising from the breakdown of the ordered, helical mammalian proteins and collagens [1,2]. Its gelation at room temperature and a relatively low concentration is well known [3]. Since the very beginning of photographic industry, gelatin has been utilized as a colloidal protective agent [4]. Nowadays, synthetic polymers have made great progress but gelatin as a abundant kind of proteins is still widely used in food and pharmaceutical industries because of its special gelling, binding, and thickening properties [5, 6]. Gelatin has previously been extensively investigated, including its sol–gel transition [7,8], phase behavior [6,9, 10], aggregation/complexation [11–13], adsorption [5, 14–18], the immunization applications [19,20], purification [21], and the stabilization of colloid particles [22].

It has been recognized that the adsorption of gelatin, an

amphoteric polyelectrolytes, on a charged surface is particularly complicated because a gelatin chain contains both anionic and cationic groups. The adsorption could be driven by electrostatic or/and by hydrophobic interaction, depending on the nature of surface and the medium. Moreover, gelatin chains can strongly interact with each other in water by hydrogen bond between amino and carboxylic groups on the chain backbone. Many previous studies were mainly focused on the effect of the ionic strength, pH and surface charge on the adsorption of gelatin [5,15,17,18]. Buffer solutions and low molar mass electrolytes were often used to maintain the ionic strength and pH.

In order to simplify the problem and to have a better understanding of the stabilization mechanism, we designed an LLS investigation on the adsorption of different types of gelatins on surfactant-free and narrowly distributed polystyrene nanoparticles. Using small particles enabled us to observe a larger relative size change after the adsorption so that the results are much more reliable. The emphasis of our study was to understand the difference between the adsorption processes driven by electrostatic and hydrophobic interactions.

* Corresponding author. Address: Department of Chemistry, The Chinese University of Hong Kong, Shatin, N.T., Hong Kong, People's Republic of China.

2. Experimental

2.1. Sample preparation

Deionized water with a resistivity of 18 MΩ cm was used. Narrowly distributed surfactant-free polystyrene nanoparticles with a nominal average diameter of ~44 nm and a polydispersity index of $\sim 1.03 \pm 0.01$ was purchased from Seradyn. According to the manufacture, an ion-exchange process was used to remove surfactant, alkylsulfonate, used in the microemulsion polymerization, which has been confirmed by electrophoretic laser light scattering (LLS). Diluting the dispersion and increasing its pH up to 11 had no effect on their stability because of negatively charged sulfate groups on the nanoparticle surface. The nanoparticle dispersion had a ζ -potential of ~ -40 mV. Four gelatin samples provided by BASF were used. Two of them were alkali-processed, respectively, denoted as gelatin-B1 and gelatin-B2. The other two were acid-processed, respectively, denoted as gelatin-A1 and gelatin-A2. Their molecular parameters are summarized in Table 1. Note that GPC and LLS led to different values of M_w . It has been known that GPC only gives an apparent value of M_w of gelatins [23]. The isoelectric points (IEP) of A- and B-type gelatins are pH $\sim 8.9 \pm 0.1$ and pH $\sim 4.9 \pm 0.1$, respectively, [1]. All the gelatin samples were used without further purification.

The gelatin stock solution was prepared by two different methods. In the first, a proper amount of gelatin was dissolved in pure water at 40 °C. The dilute gelatin solutions were kept at 40 °C for at least one day to ensure a complete dissolution. The gelatin/nanoparticle mixtures were stirred with magneton and kept in the temperature range 35–40 °C for one more day before the LLS measurements. In the other method, gelatin was first dissolved in a small amount of formamide at 25 °C, which was then transferred into a fifty-time volume of water. For all the gelatin/nanoparticle mixtures, the nanoparticle concentration was kept at 10 μg/ml and the gelatin/nanoparticle weight ratio was in the range 0.01–3.00. All the gelatin/nanoparticle dispersions were clarified by 0.5 μm millipore Millex filters.

Table 1
Characterization and molecular parameters of four gelatin samples used at 25 °C

Sample	Gelatin-B1	Gelatin-B2	Gelatin-A1	Gelatin-A2
$M_{w,GPC}$ (g/mol)	136,000	456,000	92,000	215,000
$M_{n,GPC}$ (g/mol)	56,100	60,600	39,700	83,000
$M_{w,LLS,formamide}$ (g/mol)	81,000	650,000	20,000	125,000
$\langle R_h \rangle_{formamide}$ (nm)	10.2	30.7	15	11.7
$\langle R_g \rangle_{formamide}$ (nm)	15	48	27	23
$\langle R_h \rangle_{water+formamide}$ (nm)	10.5	32	14	12.2
$\langle R_g \rangle_{water+formamide}$ (nm)	25	50	23	27
Relative width of $G(I)$	0.24	0.26	0.22	0.22
pH _{gelatin solution}	~6.1	~6.0	~6.3	~6.2

2.2. Laser light scattering

The LLS spectrometer (ALV/SP-125) has been described earlier [24]. The specific refractive index increment (dn/dC) was determined by using a novel and precise differential refractometer [25]. In static LLS, the angular dependence of the absolute excess time-averaged scattered intensity $R_{vv}(\theta)$, known as the Rayleigh ratio, was measured. For a very dilute solution, the weight average molar mass (M_w) is related to $R_{vv}(\theta)$ by [26]

$$\frac{K'(dn/dC)^2}{R_{vv}(q)} \cong \frac{1}{M_w} \left(1 + \frac{1}{3} \langle R_g^2 \rangle_z q^2 \right) \quad (1)$$

where $K' = 4\pi^2 n^2 / (N_{Av} \lambda_0^4)$ and $q = (4\pi n / \lambda_0) \sin(\theta/2)$ with N_{Av} , n and λ_0 being the Avogadro' constant, the solvent refractive index and the laser wavelength in vacuum, respectively, and $\langle R_g^2 \rangle_z^{1/2}$ (or simply $\langle R_g \rangle_z$) is the z -average root-mean-square radius of gyration. In this study, the mixture was so diluted that the extrapolation of $[R_{vv}(\theta)]_{C \rightarrow 0}$ was not necessary. Note that the light scattered from each nanoparticle was so strong that the intensities of the light scattered from water and individual non-adsorbed gelatin chains free in water could be neglected. For the adsorption, it is reasonable to consider the particle adsorbed with gelatin as a polymeric core-shell nanostructure, we were able to use a simple weight additive method to calculate dn/dC [27], i.e.

$$\left(\frac{dn}{dC} \right)_{particle+gelatin} = \chi_{gelatin} \left(\frac{dn}{dC} \right)_{gelatin} + (1 - \chi_{gelatin}) \times \left(\frac{dn}{dC} \right)_{particle} \quad (2)$$

where $\chi_{gelatin} = m_{gelatin} / (m_{adsorbed} + m_{particle})$ with $m_{particle}$ and $m_{adsorbed}$ being the macroscopic masses of the particles and the adsorbed gelatin chains, respectively. Therefore, the weight concentration (C) of the particles adsorbed with gelatin is $(m_{particle} + m_{adsorbed})/V$, or written as, $(1 + m_{adsorbed}/m_{particle})C_{particle}$, where $C_{particle} [= m_{particle}/V]$ is the particle concentration before the adsorption. The measured specific refractive index increments of the gelatin chains and the particles in water are 0.167 and 0.256 ml/g,

respectively. A combination of Eqs. (1) and (2) leads to

$$(M_w)_{\text{PS+gelatin}} = \frac{[R_{\text{vv}}(\theta)]_{\text{particle+gelatin}}}{K[(dn/dC)_{\text{particle+gelatin}}]^2 C_{\text{particle+gelatin}}} \quad (3)$$

where $[R_{\text{vv}}(q)]_{\text{particle+gelatin}}$ and $(M_w)_{\text{particle+gelatin}} \times [(1 + m_{\text{adsorbed}}/m_{\text{particle}})(M_w)_{\text{particle}}]$ are the Rayleigh ratio and the weight average molar mass of the particles after the adsorption, respectively, and $(M_w)_{\text{particle}} \times [R_{\text{vv}}(q)]_{\text{particle}}/[K'(dn/dC)_{\text{particle}}^2 C_{\text{particle}}]$ is the weight average molar mass of the particles before the adsorption. Eq. (3) can be rearranged as

$$\frac{m_{\text{adsorbed}}}{m_{\text{particle}}} = \frac{(dn/dC)_{\text{particle}}}{(dn/dC)_{\text{gelatin}}} \left\{ \left(\frac{[R_{\text{vv}}(\theta)]_{\text{particle+gelatin}}}{[R_{\text{vv}}(\theta)]_{\text{particle}}} \right)^{1/2} - 1 \right\} \quad (4)$$

where $[R_{\text{vv}}(\theta)]_{\text{particle}}$ is a constant for a given C_{particle} , dn/dC can be independently measured. $m_{\text{adsorbed}}/m_{\text{particle}}$ can be determined from $[R_{\text{vv}}(\theta)]_{\text{particle+gelatin}}$ measured in static LLS. Since knowing the average mass and size of each particle, we are able to convert $m_{\text{gelatin}}/m_{\text{particle}}$ to the average mass of the adsorbed gelatin chains ($\langle m \rangle$) per particle or the adsorption density ($\langle \sigma \rangle$) defined as $\langle \sigma \rangle = \langle m \rangle / (4\pi \langle R_{\text{h},0} \rangle^2)$, where $\langle R_{\text{h},0} \rangle$ is the average hydrodynamic radius of the particles before the adsorption. The estimate additional error of using Eq. (4) on the basis of the uncertainties of the measurement is about $\pm 5\%$.

In dynamic LLS, the cumulant analysis of the measured intensity–intensity time correlation function $G^{(2)}(\tau, \theta)$ in the self-beating mode could result in an average line-width (Γ) or a line-width distribution [28,29]. For a diffusive relaxation, $\langle \langle \Gamma \rangle / q^2 \rangle_{C \rightarrow 0, q \rightarrow 0}$ leads to the average translational diffusion coefficient ($\langle D \rangle$) or further to the averaged hydrodynamic radius $\langle R_{\text{h}} \rangle (= k_{\text{B}} T / 6\pi \eta \langle D \rangle)$, where k_{B} , T and η are the Boltzmann constant, absolute temperature and solvent viscosity, respectively. The hydrodynamic volume (V) of the PNIPAM layer adsorbed on the particle surface is related to the size difference (ΔR_{h}) between the particle after and before the adsorption by [30]

$$V = (4/3)\pi \left[\langle \langle R_{\text{h}} \rangle_0 + \Delta R_{\text{h}} \rangle^3 - \langle R_{\text{h}} \rangle_0^3 \right] \\ = (4/3)\pi \langle R_{\text{h}} \rangle_0^3 f(\Delta R_{\text{h}} / \langle R_{\text{h}} \rangle_0) \quad (5)$$

where $f(\Delta R_{\text{h}} / \langle R_{\text{h}} \rangle_0) = 3(\Delta R_{\text{h}} / \langle R_{\text{h}} \rangle_0) + 3(\Delta R_{\text{h}} / \langle R_{\text{h}} \rangle_0)^2 + (\Delta R_{\text{h}} / \langle R_{\text{h}} \rangle_0)^3$. It can be seen that using small nanoparticles enabled us to accurately determine ΔR_{h} and V .

3. Results and discussion

Fig. 1 shows the adsorption of gelatin-B1 on the nanoparticles in pure water (pH ~ 6.5). The thickness of the adsorbed gelatin layer ($\Delta \langle R_{\text{h}} \rangle$) increases as the adsorption increases. Experimentally, we found a maximum when $(m_{\text{adsorbed}}/m_{\text{particle}})_{\text{max}}$ was close to ~ 0.34 or the

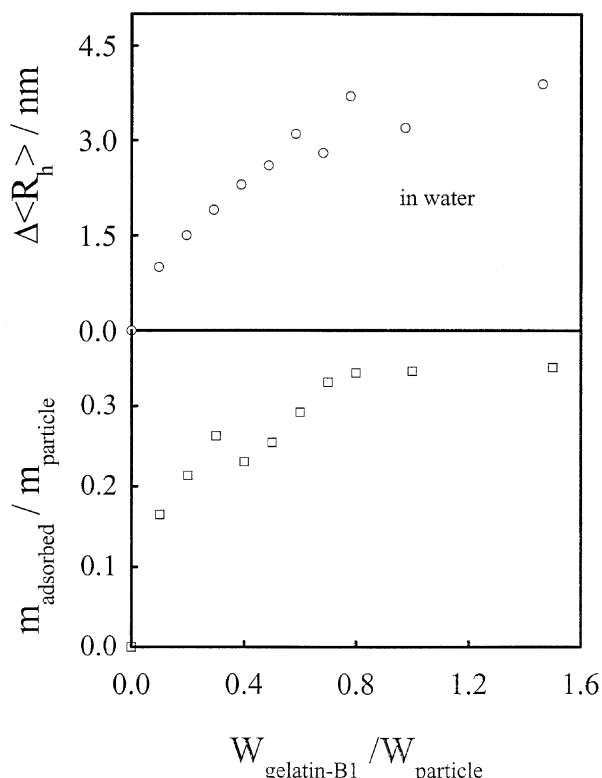


Fig. 1. Relative gelatin concentration ($W_{\text{gelatin-B1}}/W_{\text{particle}}$) dependence of hydrodynamic thickness ($\Delta \langle R_{\text{h}} \rangle$) and the relative adsorption ($m_{\text{adsorbed}}/m_{\text{particle}}$) for gelatin-B1 adsorbed on polystyrene nanoparticles in pure water at 25 °C, where the nanoparticle concentration was kept at 1.00×10^{-5} g/ml. $\Delta \langle R_{\text{h}} \rangle = \langle R_{\text{h}} \rangle - \langle R_{\text{h},0} \rangle$ with $\langle R_{\text{h},0} \rangle$ and $\langle R_{\text{h}} \rangle$ are the average hydrodynamic radii of nanoparticles after and before the adsorption, respectively. $W_{\text{gelatin-B1}}$ and W_{particle} are macroscopic weights of gelatin and nanoparticles added in the dispersion. m_{adsorbed} and m_{particle} are the masses of the gelatin chains adsorbed and polystyrene nanoparticles used.

adsorption density (σ) reached ~ 2.5 mg/m². According to Table 1, the maximum thickness was still smaller than the chain size of non-adsorbed gelatin molecules free in solution, indicating that the adsorption was monolayer. In pure water (pH ~ 6.5), the overall B-type gelatin chain is slightly negatively charged due to the ionization of carboxylic acid groups. However, the adsorption is not prevented by the repulsion between negatively charged particle surface and groups on the gelatin chains. This is because the gelatin chain also carries positively charged amide groups. This phenomenon has previously been reported for both the adsorption and complexation of gelatin chains in solution [5,12,32–35].

Fig. 2 shows that the average hydrodynamic volume (V_{shell}) of the adsorbed gelatin layer (the shell) on each nanoparticle is a linear function of the amount of the gelatin adsorbed on the nanoparticle surface. It reveals that the adsorbed gelatin layer has a constant density of ~ 0.36 g/cm³, much higher than the density (~ 0.03 g/cm³) of individual swollen gelatin chains free in solution, but close to that of a collapsed polymer chain [36,37]. In a

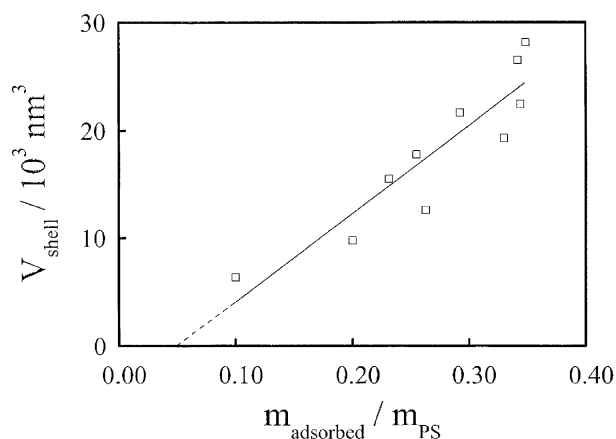


Fig. 2. Relative adsorption ($m_{\text{adsorbed}}/m_{\text{particle}}$) dependence of average hydrodynamic volume (V_{shell}) of the gelatin layer adsorbed on each polystyrene nanoparticle in pure water at 25 °C, where the nanoparticle concentration was kept at 1.00×10^{-5} g/ml, $V_{\text{shell}} = (4\pi/3)(\langle R_h \rangle^3 - \langle R_h \rangle_0^3)$ with $\langle R_h \rangle_0$ and $\langle R_h \rangle$ being the average hydrodynamic radii of polystyrene nanoparticles before and after the adsorption of gelatin. Other variables are the same as in Fig. 1.

previous study of the hydrophobic adsorption of flexible poly(*N*-isopropyl acrylamide) (PNIPAM) chains on the nanoparticles [30], we found that V_{shell} is proportional ($m_{\text{adsorbed}}/m_{\text{particle}}$) [2]. The difference can be attributed to the fact that the adsorption of gelatin on the negatively charged nanoparticles is driven by electrostatic interaction; namely, such strong electrostatic attraction forces the gelatin chains to lie flatly on the nanoparticle surface.

Our results also showed that when longer gelatin chains (gelatin-B2) were used, the adsorption saturation was reached at a much lower gelatin/particle weight ratio. The adsorbed gelatin layer was thicker for a given amount of the adsorption ($m_{\text{adsorbed}}/m_{\text{particle}}$), indicating that longer gelatin chains can form larger loops on the surface and were more effective in the surface coverage. It should be stated that in water solutions the adsorption of longer gelatin chains often resulted in the flocculation, other than the stabilization, of the nanoparticles in the dispersion because strong and long range electrostatic interaction between the nanoparticles and gelatin chains made the longer gelatin chains to act as ‘bridges’ even though the nanoparticle concentration was as low as 1.00×10^{-5} g/ml [38,39]. The flocculation became more obvious when the cationic A-type gelatin chains at pH ~ 6.5 was used.

In order to reduce the electrostatic interaction, low molar mass salts, such as NaCl and KSCN, are often used to screen out the electrostatic interaction and break hydrogen bonding [11,40,41]. However, we found that KSCN and other added salts induced the flocculation, i.e. the salt-out effect, because the nanoparticles are stabilized by electrostatic interaction. We were caught between the screening of electrostatic interaction and the stabilization of the nanoparticles. We also found that the variation of pH had nearly no help in stabilizing the gelatin/nanoparticle mixture. Finally, we used formamide, an organic co-solvent, because it is a good

solvent for gelatin at room temperature [40,41]. Our results showed that all the four gelatin samples could form concentrated formamide solutions up to 10% at ~ 22 °C without gelation, which is attributed to a similarity between formamide and the peptide linkages in the chain backbone of gelatin; namely, formamide can interact with gelatin by a rather specific and chelated solvation in terms of a cyclic dimerization of carboxylic acids and amides [38]. The characterization of all the gelatin samples in formamide were also summarized in Table 1. The formamide solution was diluted with an excess of water to form a gelatin aqueous solution with only 2 wt% of formamide. The LLS results of the four gelatins in the water/formamide mixture are also listed in Table 1. The results in pure formamide and the water/formamide mixture are comparable. The ratios of $\langle R_g \rangle / \langle R_h \rangle \sim 1.5$ indicate that the gelatin chains have a coil conformation.

Fig. 3 shows that in the presence of 2 wt% formamide, the gelatin chains adsorbed on the nanoparticle were much more extended in comparison with Fig. 1. The chelation between the gelatin chain and formamide makes gelatin act as a neutral polymer. It switches the main driving force of the adsorption from electrostatic to hydrophobic. Fig. 3 also shows that the adsorption was nearly independent of the mixing temperature. For the longer chain gelatin-B, the maximum thickness of the adsorbed gelatin layer reached

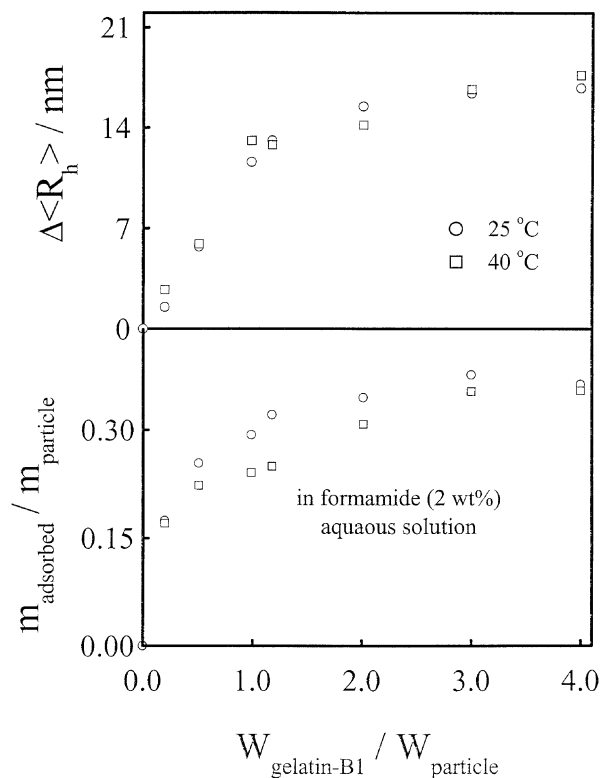


Fig. 3. Relative gelatin concentration ($W_{\text{gelatin-B1}}/W_{\text{particle}}$) dependence of hydrodynamic thickness ($\Delta\langle R_h \rangle$) and the relative adsorption ($m_{\text{adsorbed}}/m_{\text{particle}}$) for gelatin-B1 adsorbed on polystyrene nanoparticles at 25 °C in 2 wt% formamide aqueous solution, where the nanoparticle concentration was kept at 1.00×10^{-5} g/ml. Other variables are the same as in Fig. 1.

~40 nm at $m_{\text{polymer}}/m_{\text{particle}} \sim 0.45$. The variation of pH in the range 6.0–8.5 had no detectable influences on the adsorption, indicating that electrostatic interaction was suppressed in the presence of only 2 wt% formamide. There was nearly no difference between the adsorption of the A- and B-type gelatins in the water/formamide mixture.

Fig. 4 shows a better view of the nature of the adsorption; namely, V_{shell} is proportional to $(m_{\text{adsorbed}}/m_{\text{particle}})^2$ for all the four gelatin samples, a characteristics of the hydrophobic adsorption of long linear polymer chains on surface. Note that m_{adsorbed} is proportional to the average number (n_{chain}) of the gelatin chains adsorbed on each nanoparticle and m_{particle} is a constant. Also note that the volume per adsorbed chain (v_{chain}) is proportional to $V_{\text{shell}}/n_{\text{chain}}$. Therefore, on the basis of the experimental results, we have $V_{\text{shell}} \propto n_{\text{chain}}^2$ and $v_{\text{chain}} \propto n_{\text{chain}}$. It is reasonable to assume that the total number of the adsorbing sites available on each particle remains a constant. For each adsorption point, there exists a dynamic equilibrium between the adsorption and desorption. When more polymer chains are presented in the dispersion, it is more likely that the adsorbing site released by one adsorbed chain is occupied by another non-adsorbed chain originally free in the dispersion. Therefore, the average number of the adsorbing sites per chain on the surface decreases as the gelatin

concentration increases. In this way, the average chain segment length between two neighboring adsorbing sites, i.e. the length of a ‘loop’, increases with the gelatin concentration. This explains why v_{chain} increase with n_{chain} . In the case of electrostatic adsorption, the strong attraction makes the desorption much more difficult so that the volume per adsorbed gelatin chain remains a constant, independent of the gelatin concentration. It should be addressed that the above qualitative discussion is independent of a particular polymer/particle system. It should be noted that in Fig. 4, the adsorption of the A-type gelatin leads to the lines passing the zero point, but not the adsorption of the B-type gelatin. It indicates that when the adsorption is low, the B-type gelatin chains are flatly adsorbed on the particle surface so that they have a very small contribution to $\langle R_h \rangle$.

Fig. 5 shows that $\langle R_h \rangle$ is less sensitive to pH, but the adsorption for both the gelatin/nanoparticle mixtures were higher when pH was too low or too high. It is expected that at a lower pH, the A-type gelatin chains are cationic, resulting in a stronger electrostatic attraction between the chains and negatively charged nanoparticle surface, resulting in a stronger adsorption, while at a higher pH, the A-type gelatin chains are near its isoelectric point so that they are not stable in water, which normally leads to a high adsorption [5,14,31]. Note that for gelatin-A2 at pH ~9.7, the adsorption is much higher, but not $\langle R_h \rangle$. This indicates that the adsorption of long gelatin chains on the nanoparticle

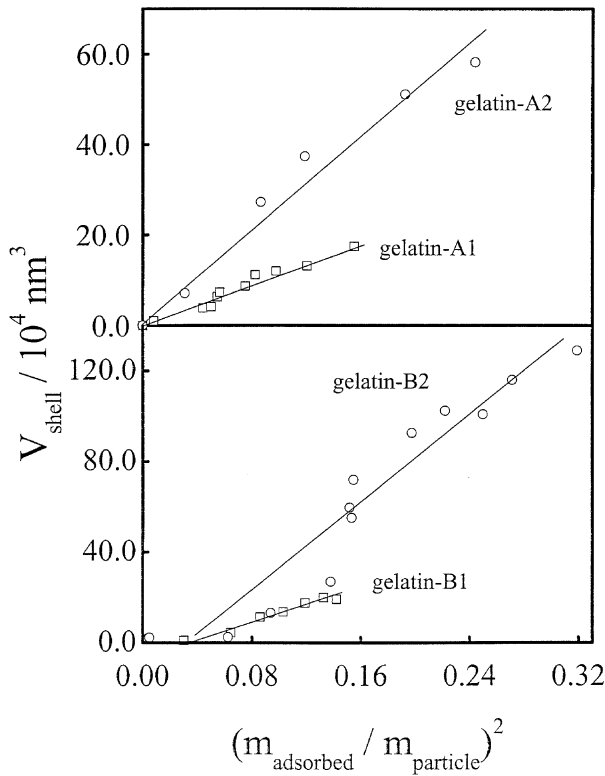


Fig. 4. Relative adsorption ($m_{\text{adsorbed}}/m_{\text{particle}}$) dependence of average hydrodynamic volume (V_{shell}) of the gelatin layer adsorbed on each polystyrene nanoparticle in a water/formamide (2 wt%) mixture at 25 °C, where the nanoparticle concentration was kept at 1.00×10^{-5} g/ml. The lines represent the least square linear fittings of V_{shell} (nm^3) versus $(m_{\text{adsorbed}}/m_{\text{particle}})^2$. Other variables are the same as in Fig. 1.

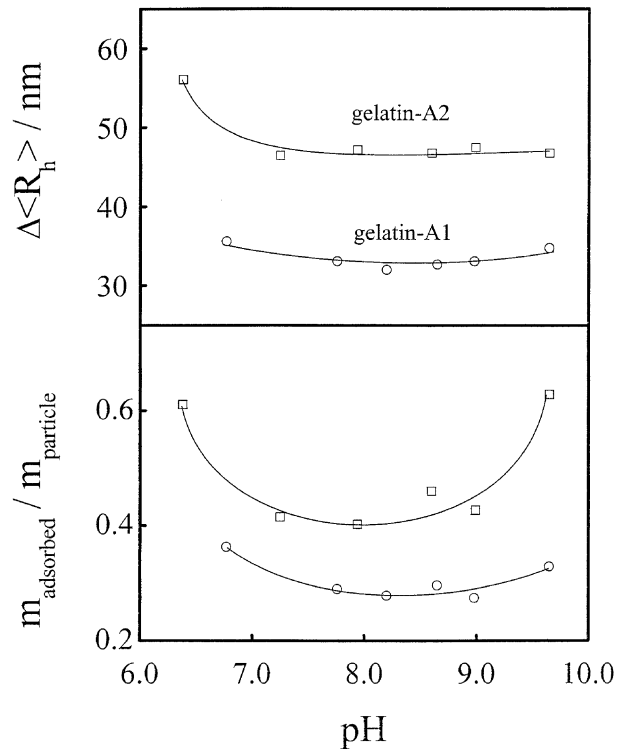


Fig. 5. pH dependence of average hydrodynamic gelatin layer thickness ($\Delta\langle R_h \rangle$) and relative adsorption ($m_{\text{adsorbed}}/m_{\text{particle}}$) at 25 °C in a formamide (2 wt%) aqueous solution, where the concentrations of gelatin and polystyrene nanoparticles were kept at 2.00×10^{-5} and 1.00×10^{-5} g/ml, respectively. Other variables are the same as in Fig. 1.

surface resulted in a higher chain density, but not the thickness of the adsorbed layer. Such a result has an implication in the formulation of stable nanoparticles because the adsorbed layer thickness, not the amount of the adsorbed gelatin, plays a key role in the stabilization. This result tells us that when one uses A-type gelatin in the stabilization, pH should be controlled in the range 7–9.

4. Conclusion

Our results showed that in pure water, the adsorption of gelatin on negatively charged polystyrene nanoparticles was mainly driven by electrostatic attraction. Such attraction was so strong that the mixing of the A-type gelatin (cationic in pure water) with the nanoparticles could easily result in an interparticle aggregation because one gelatin chain adsorbed on two nanoparticles can bridge them together, especially when long gelatin chains were used. On the other hand, the electrostatic attraction induced the collapse of the chain on the nanoparticle surface so that the adsorbed gelatin layer was denser. The addition of 2 wt% formamide into water could effectively suppress the electrostatic interaction and break the hydrogen bonding between the gelatin chains because of a special chelation between formamide and the carbonic and amide groups on the gelatin chains. Therefore, the dominant interaction in the adsorption switched from electrostatic to hydrophobic. Such a change was evidenced by the change of the scaling between the relative adsorption ($m_{\text{adsorbed}}/m_{\text{particle}}$) and the hydrodynamic volume (V_{shell}) of the gelatin layer on the particle surface; namely, from $V_{\text{shell}} \propto m_{\text{adsorbed}}/m_{\text{particle}}$ to $V_{\text{shell}} \propto (m_{\text{adsorbed}}/m_{\text{particle}})^2$, where m_{adsorbed} is the average mass of the gelatin chains adsorbed on each nanoparticle and m_{particle} is the average mass per nanoparticle. It is known that formamide is only minor poisonous and bio-compatible to organism. Therefore, formamide could be used as an auxiliary agent of gelatin to stabilize colloidal dispersions in pharmaceutical and food industry.

Acknowledgments

The financial support of the BASF-Sino-German Research & Development Fund (1998), the Research Grants Council of Hong Kong Special Administrated Region Earmarked Grant 1997/98 (CUHK4266/OOP, 2160135) (CUHK4257/OIP, 2160174) and the CAS Bai Ren Project are gratefully acknowledged.

References

- [1] Veis A. The macromolecular chemistry of gelatin. London: Academic Press; 1964.
- [2] Ward A, Courts A, editors. The science and technology of gelatin. London: Academic Press; 1977.
- [3] Dickinson E, Lam WL-K, Stainsby G. Colloid Polym Sci 1984;262: 51.
- [4] Cox RJ. Photographic gelatin. London: Academic Press; 1972.
- [5] Kamiyama Y, Israelachvili J. Macromolecules 1992;25:5081.
- [6] Clewlow AC, Clarke AH, Rowe AJ, Tombs MP. Biochem Soc Trans 1995;23:498.
- [7] Wu DQ, Chu B. Mol Res Soc Symp Proc 1992;143:203.
- [8] Cho M, Sakashita H. J Phys Soc Jpn 1996;65:2790.
- [9] Tromp RH, Rennie AR, Jones RAL. Macromolecules 1995;28:4129.
- [10] Tromp RH, Jones RAL. Macromolecules 1996;29:8109.
- [11] Helga B, Paul D. J Phys Chem 1954;58:968.
- [12] Bowman WA, Rubinstein M, Tan JS. Macromolecules 1997;30:3262.
- [13] Griffiths PC, Stilbs P, Howe AM, Cosgrove T. Langmuir 1996;12: 2884.
- [14] Thomas M, Kellaway IW, Jones BE. Int J Pharmacol 1991;73:185.
- [15] Muller D, Malmsten M, Bergenstahl B, Hessing J, Olijve J, Mori F. Langmuir 1998;14:3107.
- [16] Haugstad G, Gladfelter WL, Weberg EB, Weberg RT, Weatherill TD. Langmuir 1994;10:4295.
- [17] Kawanishi N, Christenson HK, Ninham BW. J Phys Chem 1990;94: 4611.
- [18] Kudish AT, Eirich FR. ACS Symp Ser 1987;343:261.
- [19] Schramm W, Paek SH. Anal Biochem 1992;205:47.
- [20] McGinlay PB, Bardsley WG. Biochem J 1989;261:715.
- [21] Regnault V, Rivat C, Stoltz JF. J Chromatogr 1988;432:93.
- [22] Papadimitrakopoulos F, Wisniecki P, Bhagwagar DE. Chem Mater 1997;9:2928.
- [23] Wu C. Macromolecules 1993;26:5423.
- [24] Gao J, Wu C. Macromolecules 1997;30:6873.
- [25] Wu C, Xia KQ. Rev Sci Instrum 1994;65:587.
- [26] Zimm BH. J Chem Phys 1948;16:1099.
- [27] Xia J, Dubin P. In: Dubin P, Bock J, Davies RM, Schulz DN, Thies C, editors. Macromolecular complexes in chemistry and biology. Berlin: Springer; 1994. p. 247.
- [28] Berne BJ, Pecora R. Dynamic light scattering. New York: Wiley; 1976.
- [29] Chu B. Laser light scattering: basic principles and practice. London: Academic Press; 1991.
- [30] Gao J, Wu C. Chin J Polym Sci 1999;17(6):595.
- [31] Akihiko K, Ko H. J Colloid Interf Sci 1992;150:344.
- [32] Brown W, Zhao JX. Macromolecules 1993;26:2711.
- [33] Park JM, Muhoherac BB, Dubin PL, Xia J. Macromolecules 1992;25: 290.
- [34] Xia J, Dubin PL, Kim Y, Muhoherac BB, Klimkowski VJ. J Phys Chem 1993;97:4528.
- [35] Ahmed LS, Xia J, Dubin PL. J Macromol Sci, Pure Appl Chem 1994; A31:17.
- [36] Curme HG, Natale CC. J Phys Chem 1964;68:3009.
- [37] Berendsen R, Borginon H. J Photogr Sci 1968;16:194.
- [38] Pelton R, Xiao HN, Brook MA, Hamielec A. Langmuir 1996;12:5756.
- [39] Rustemeier O, Killmann E. J Colloid Interf Sci 1997;190:360.
- [40] Stejskal J, Strakova D, Kratochvil P. Makromol Chem 1987;188:855.
- [41] Wu C. J Polym Sci, Part B: Polym Phys 1995;32:803.